iJRASET
International Journal For Research in Applied Science and Engineering Technology

INTERNATIONAL JOURNAL FOR RESEARCH

IN APPLIED SCIENCE & ENGINEERING TECHNOLOGY

Volume: 6 **Issue:** VII **Month of publication:** July 2018

DOI: http://doi.org/10.22214/ijraset.2018.7018

www.ijraset.com

Call: 08813907089 | E-mail ID: ijraset@gmail.com

International Journal for Research in Applied Science & Engineering Technology (IJRASET)
ISSN: 2321-9653; IC Value: 45.98; SJ Impact Factor: 6.887
Volume 6 Issue VII, July 2018- Available at www.ijraset.com

Optimization of Impingement Cooled Heat Sink using Experimental and CFD Simulation Methods

ShantanuVedpathak[1], Dr. Ankur Saxena[2], Dr. Kiran C. More[3]
[1]*P.G. Student, Mechanical Engineering Department, D Y Patil School of Engineering Academy, Pune, Maharashtra, India*
[2]*HOD, Department of Automobile Engineering, D Y Patil School of Engineering Academy, Pune, Maharashtra, India*
[3]*PG Coordinator, D Y Patil Institute of technology, Ambi*

Abstract: ***Impingement cooling method utilizes high speed jet(s) to impinge on a high temperature surfaces for cooling or heating. In this study, various heat sink geometrical configurations – Heat sink with no fins, Heat sink with continuous plate-fins, Heat sink with interrupted plate-fins, Heat sinks with pin-fins – were studied. The studies had been conducted for three jet velocity (2, 4 and 6 m/s) as well as three Z/d ratio of 2, 4 and 6. Numerical simulations for this work had been performed in ANSYS FLUENT with RNG k-ϵ turbulence model to account for the Reynolds Stresses. Experimental studies had been conducted to validate the predictions from the CFD simulations. As high as 25% heat transfer enhancement was observed by employing pin-fins. The ineffectiveness of the plate fins –both continuous and interrupted – for the impingement cooling were attributed to obstruction to the flow path in these geometrical variants. Also, the increase in the pin-fin diameter was resulted heat transfer enhancement.***

Keywords: Jet Cooling, Impingement Cooling, Heat Sink CFD, Single-Jet Impingement, Heat Transfer Enhancement.

I. INTRODUCTION

Impingement cooling or jet cooling works on the principle of injecting high speed jets on to a heat source / heat sink. Since the high speed jets contain high heat fluxes, this method ensures higher heat transfer between the fluid and the heat source. When the high speed jet impinges on a flat plate heat source, such as shown in the following figure 1 (MdLokmanHosain, 2014), the flow profile could be divided in to the five zones.

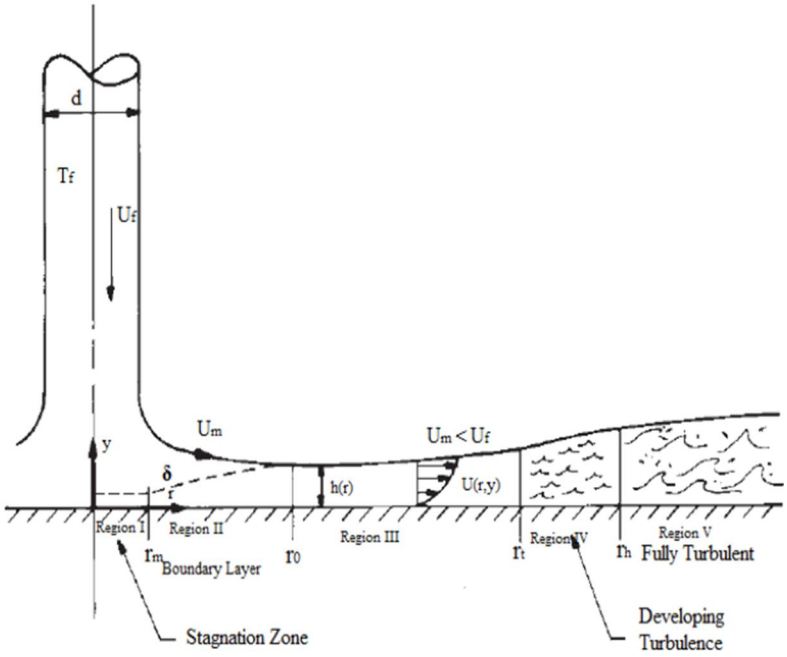

Figure 1: Schematic explanation of flow profile in impingement cooling (MdLokmanHosain 2014)

A. *Region I – Stagnation Zone*

1) Stagnation zone occurs at the impingement point and the kinetic energy of the jet will be converted to the pressure energy.

2) So, in this zone, the fluid would contain typically very high pressure energy and would be remain nearly stagnant

B. Region II – Laminar Boundary Layer

1) After the impingement, (Region I) the coolant fluid moves in outward direction (radially / tangentially)

2) During this phase, the flow boundary will be developed on the heat source surface (impinging surface).

3) However, in this zone, the flow boundary layer (δ) is smaller than the liquid film thickness h(r)

C. Region III – In this zone, the flow boundary layer reaches the height of film surface

D. Region IV – Transition Region

1) Here, both the flow and thermal boundary layer both develop to the height of the liquid surface

E. Region V – Fully turbulent region

1) In this zone, the coolant flow velocity is reduced as compared to the jet' velocity

2) Also, the flow becomes fully turbulent in this zone.

When the high speed jet hits a wall surface, the fluid pressure will increase at the impact location which forces the fluid acceleration from there towards outward direction in a thin liquid film. This fluid film usually of millimeters in thick and typically covers the wall surface. The skin friction effect between the fluid and wall results in boundary layer and the temperature difference results in thermal boundary layer. With the formation of this thin layer, the heat transfer between the high temperature walls to the typically colder fluid takes place hence the heat removal mechanism is established.

II. LITERATURE SURVEY

Hussein M Maghrabie(2016)had conducted jet impingement in cross flow (JICF) for the representation of electronic components using CFD simulations in ANSYS FLUENT. They had observed significant changes in heat transfer between jet impingement in cross flow (JICF) and estimated a 26% increase for the jet impingement in cross flow. The influence of fan-exit-to-impingement distance on the heat transfer enhancement with impingement cooling was studied by D Sui (2008). They had concluded that with the increase in the clearance ratio, the heat transfer rate was found to be reducing. The pressure profiles on the heat sink for the jet cooling was studied Malladi R ChSastry (2015)for multiple jet impingement cooling model. A secondary peak was located between the impinging jets by the authors in their study. Also, it was found that the secondary pressure peak to be independent of the flow Reynolds number. For performing the CFD simulations, most commonly used method was Reynolds Averaged Navier Stokes (RANS) approach to model the Reynolds Stresses. N Zuckerman (2006) had in their studies identified v2-f turbulence model to provide accurate results as compared to other turbulence models. The investigation of utilizing the nano-particles such as Al2O3 for the jet impingement cooling was studied by Jun-Bo Huang (2013). For modeling these two-phase materials (Water + Al2O3) in the CFD simulations, the authors had employed the mixture multi-phase model in their simulations. Based on the obtained results, they had observed a heat transfer enhancement of 10-15% for 5% nanoparticles in the impinging fluid. The influence of the impinging fluid's turbulence level was investigated by M. Behnia (2005). In their research work, the authors had shown that the numerical predictions of heat transfer rates are very sensitive to turbulence model and the wall treatment. Marcelo J S de Lemos (2008) had analyzed the impingement cooling method for a porous material. The metal porous foam was placed on top of the hot surfaces while laminar impinging jet was utilized for cooling. The porous metal foam height, permeability was varied in their study. This was simulated by the authors using SIMPLE algorithm to model the pressure-velocity coupling in CFD. Zhang Jingzhou (2009) had had applied the impingement / effusion cooling methods on parallel plates with a focus on gas turbine balde cooling. In their study, the impingement cooling holes were maintained at 30° in reference to the surface, the blowing ratio and the ratio of the center-to-center distance of adjacent holes-to-hole diameter were varied in their study. Based on the results obtained, they had observed that the decreasing the center-to-center distance of holes had improved wall cooling effectiveness. This could be applied for multi-jet impingement cooling.

MdLokmanHosain (2014) had applied impingement cooling method for Runout Table (ROT) cooling with water – below the boiling point temperature – as fluid.

For CFD simulations, the author had explored 2-D axisymmetric as well 3D modeling approach with RANS turbulence models. The authors had conducted this study with single and two jets for identical operating conditions. For modeling the air (atmospheric fluid) and the water (jet fluid) interfaces in the CFD simulations, the Volume of Fluid (VoF) was chosen by the authors. Their CFD simulation results were compared with the analytical / empirical correlations and found to be acceptable.

The influence of curvature over the jet impingement cooling was studied using CFD simulations by A M Tahsini (2012). They had conducted the studies for three geometrical variants – flat plate, convex and concave impinging surface. The radiuses of curvature for convex and concave impinging surface were kept identical. The studies were extended for three different curvature ratios – 1.5,

2.0 and 2.5. For the identical operating conditions, the convex surface had highest Nusselt number at the stagnation point followed by flat plate and concave surface. For both convex and concave surfaces, the Nusselt number reduces significantly in the lateral direction as compared to the stagnation point. This was more severe in convex surfaces. The application jet impingement cooling for the aircraft wing' anti-icing was studied experimentally by Xueqin Bu (2015). So, a variable-curvature concave surface was considered by the authors for a high speed jet (Re = 21,021 to Re = 85,340) in their study. The authors had investigated the impact of the circumferential angle of the jet holes (-60° to 60°) on the piccolo tube. From the results, they had concluded that the decrease in the curvature radius and the increase in the jet impingement angle result in enhanced heat transfer. The application of jet impingement for turbine blade cooling was studied by Abdulla R Al Ali (2015) using CFD simulations. In this case, the geometry was of concave shaped surface rather than the flat plate as had been studied by various authors. The air injection velocity was varied from 5 – 65 m/s by the authors. Based on the temperature contour plots from the simulations, they concluded that the vortex created by the jet impingement on the turbine blade surfaces suppress the flow and thermal boundary layers due to the mainstream flow and hence helped in maintaining lower surface temperature.

Most of research on impingement cooling was performed with either Air or Water as fluid. However, Santosh Kumar Nayak (2016) had conducted experimental studies to analyze the impact of dual phase (Water + Air) fluid jet as impingement cooling on a heat sink. They had varied the air and water injection pressure and thereby mass flow rate of the respective fluid in their study. They had reported a maximum cooling rate of 305.1 °C/s which were far higher than obtained from the single phase jet impingement cooling methods.

III. PROBLEM STATEMENT

This project is based on the research carried out by Ridvan Yakut (2016) on the heat sink with hexagonal shaped fins. The heat sink was of square shape with the dimensions were 305 mm X 305 mm. The side length of hexagonal fins was 14 mm while the authors had studied for various fin heights (100 mm, 200 mm and 300 mm).

In their experiments, the authors have used the nozzle diameter of 50 mm for the jets. The jet velocity was varied from 4 m/s to 9 m/s for every 1 m/s interval. Based on these inputs, the project parameters were finalized and are tabulated below.

Table 1: Heat sink dimensions

Parameter	Dimension
Heat sink	305 mm X 305 mm
Jet velocity	4 m/s
Nozzle diameter	50 mm

Thermal load for the heat sink would be applied at the bottom surface. The temperature of this wall was maintained at constant temperature of T_{wall} = 75 C.

The project work considered for three impinging jet velocity of 2 m/s, 4 m/s and 6m/s to compare with the reference work. The impinging fluid will be at room temperature (T_{∞} = 30 C). Also, the project objectives were extended to investigate the impact of the nozzle-exit-to-the-impinging surface ratio, denoted as Z/d ratio here, for all the heat sink designs. So, the following were the objectives of this project work

1) Study the influence of Z/d ratio over the heat transfer enhancement from the impingement cooling
2) Study the impact of impinging jet velocity over the heat transfer rate for the impingement cooling method
3) Study the impact of pin-fins diameter on the impingement cooling method
4) Compare the Plate-fin heat sink with the base model (without any fins)

ISSN: 2321-9653; IC Value: 45.98; SJ Impact Factor: 6.887
Volume 6 Issue VII, July 2018- Available at www.ijraset.com

Ridvan Yakut (2016)had used hexagonal shaped fins in their heat sink for the experiments.

Table 2: Fin surface area calculations

Cross-sectional area of hexagon	472.54 mm^2
Fin height	100 mm
Hexagon side length	14 mm
Area of fin side surface	8400 mm^2
Total fin area from 1 hexagon fin	8872.54 mm^2
Total number of fins	18
Total surface area from fins	159,705.72 mm^2

In this present study, various fin shapes were studied for the equivalent fin surface area. Sample calculations are shown below.
The following six configurations were studied in this study
Base Model (No fins on the heat sink plate)
Variant 1: Heat Sink with Continuous Plate Fins
Variant 2: Heat Sink with Interrupted Plate Fins
Variant 3: Heat Sink with Pin-fins of diameter 10 mm
Variant 4: Heat Sink with Pin-fins of diameter 15 mm
Variant 5: Heat Sink with Pin-fins of diameter 20 mm

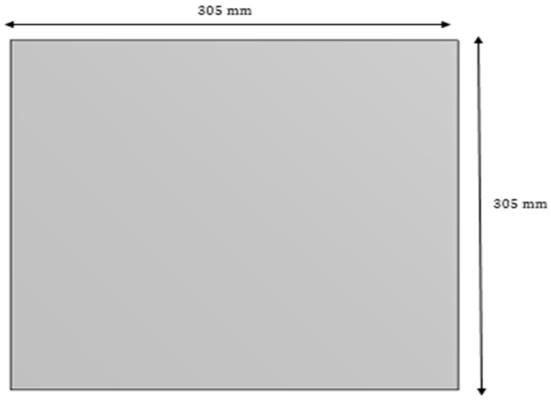

Figure 2: Base Model heat sink geometry

Variant 1 and 2 would provide insight into the effectiveness of the plate-finned heat sink under the impingement cooling while variant 3-5 would provide the impact of the pin-fin's diameter for the impingement cooling. The heat sink design calculations are provided below.
From the research work of Ridvan Yakut (2016), the total available fin area 159,705.72 mm^2(refer Table 2). So, an optimum heat sink must be designed with either an equal area or less than this.

A. Calculations for the Plate Finned Heat Sink
The height of the fins = 15 mm
Length of the plate fins = 305 mm (same as the heat sink plate)
Plate fin thickness = 2 mm

ISSN: 2321-9653; IC Value: 45.98; SJ Impact Factor: 6.887
Volume 6 Issue VII, July 2018- Available at www.ijraset.com

So, the total heat transfer surface area / plate fin = 13,785 mm^2
Number of fins = 159,705.72 / 13,785 = 11.6 ≅ 12
The geometry was generated in ANSYS Design Modeler for performing the CFD simulations and had been shown in figures 3-5.
For the Variant 2, the plate fins were made to be discontinuous by introducing the interruptions. The fin interruption of 40 mm was studied for this project. Although varying fin interruptions were decided for this research work, it was found out that the plate fins were less effective than the pin-fins for the impingement cooling. So, only one configuration of fin interruption (40 mm) was considered (Figure 4)

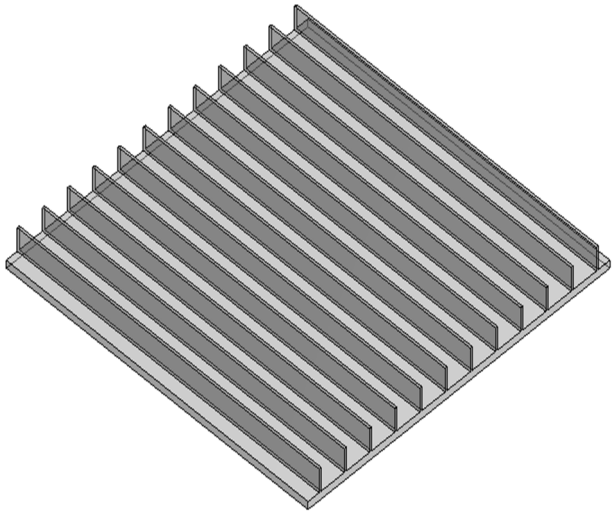

Figure 3: Heat sink of plate fins (Variant -1)

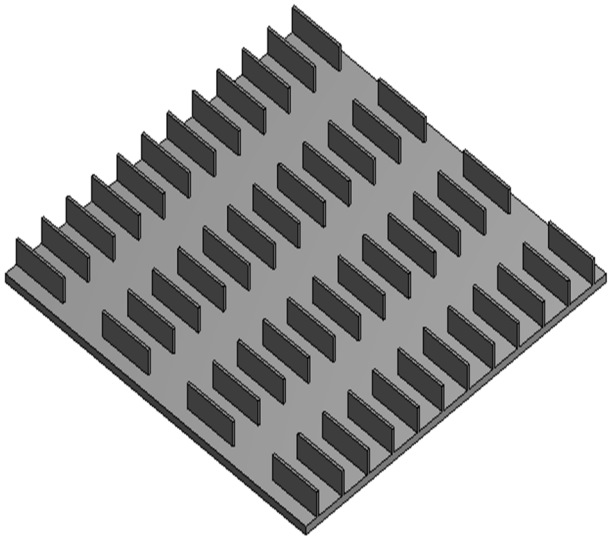

Figure 4: Heat sink of plate fins (Variant -2)

B. Pin-Finned Heat Sink (Variants 3 -5) Design:
The height of the fins = 15 mm
Fin diameter = 10 mm
Total fin surface area = 549.8 mm^2
Number of fins = 159,705.7/549.8 = 290

ISSN: 2321-9653; IC Value: 45.98; SJ Impact Factor: 6.887
Volume 6 Issue VII, July 2018- Available at www.ijraset.com

However, this would result in much closed spaced fins and that would reduce the heat transfer effectiveness. So, the material savings in heat sink material – by utilizing lesser than the available hexagonal shaped fins – was investigated. Three configurations of pin fins with 30%, 45% and 60% of the available area were designed. The final dimensions are provided below table.

Table 3: Pin-finned heat sink details

Parameters	Variant-3	Variant-4	Variant-5
Area	~30% of the available area	~45% of the available area	~60% of the available area
Pin-fin height	15 mm	15 mm	15 mm
Number of fins	81	81	81
Pin-fin diameter	10 mm	15 mm	20 mm

Number of fins was chosen to be identical for the variant 3 – 5 for maintaining geometrical consistency and minimize any impact of the variations in geometry over the heat transfer enhancement. In the following figure, the heat sink for the variant 4 had been shown. Since the variants 3, 4 and 5 were geometrically identical; the remaining two variants hadn't been shown here.

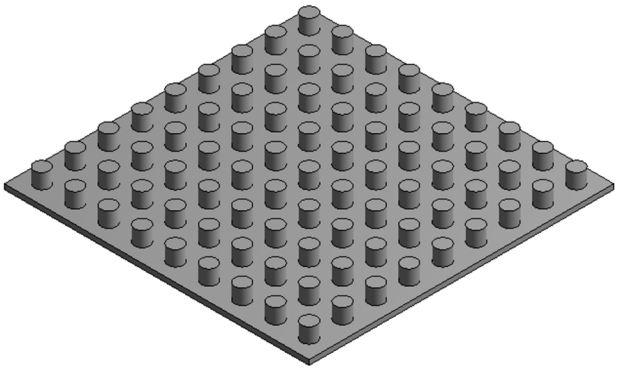

Figure 5: Heat sink of plate fins (Variant -4)

The numerical (CFD) and the experimental studies were conducted for these configurations for the flow and thermal conditions that were mentioned earlier.

IV. PROJECT METHODOLOGY

Computational Fluid Dynamics (CFD) methodology was applied in this project work to conduct the initial heat sink optimization. Once the optimal heat sink design had been identified based on the simulations, experimental studies were conducted to produce the validation between these two methodologies.

ISSN: 2321-9653; IC Value: 45.98; SJ Impact Factor: 6.887
Volume 6 Issue VII, July 2018- Available at www.ijraset.com

Figure 6: Experiment setup

Base Model heat sink was studied experimentally. The specimen (305 mm X 305 mm) was placed. The nozzle was kept at the centroid of the heat sink. This nozzle was connected to a blower whose speed could be varied and hence the flow rate was also varied as per the requirements. Heat supply was provided at the bottom of the heat sink and constant temperature was maintained (75 C). As the blower starts the operation, the jet velocity was measured. After ensuring the nozzle velocity at the respective operating conditions (2, 4 and 6 m/s) by adjusting the blower speed, the heat supply to the heat sink was monitored and the readings (Voltage and Current) were noted in the observation table. From these readings, the heat transfer rates were calculated and were compared with the CFD simulations.

Table 4: Heat Transfer Rate from Experiments

Z/d	Jet Velocity 2 m/s	Jet Velocity 4 m/s	Jet Velocity 6 m/s
2	66.2	111.8	159.3
3	68.1	121.1	168.2
4	69.4	138.4	189.1

Same procedure was repeated for the optimal heat sink variant as well.

The CFD simulations for this research work were conducted using *ANSYS Work Bench* and its various modules such as *Design Modeler, FLUENT*. The geometry was generated in Design Modeler while *ANSYS Mesher* had been utilized for computational domain discretization.

A sample snapshot of the meshing had been shown in figure 7. Typically, the mesh count for this project was ~2,800,000. The mesh count was varying as the geometry was changed among the variants. The inflation layers were applied to predict the flow gradients in the boundary layer zones.

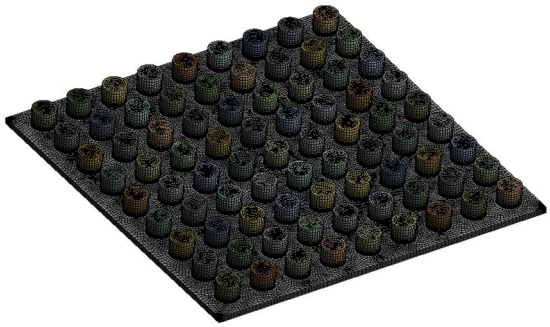

Figure 7: Meshing for the pin-fin heat sink variant

CFD simulations were conducted in *ANSYS FLUENT* with RNG k-ϵ turbulence model with enhanced wall treatment. The flow entry was modeled using velocity-inlet boundary conditions. In these simulations, the heat conduction in the Heat Sink and the convection heat transfer from solid to the surrounding fluid was modeled (conjugate heat transfer).

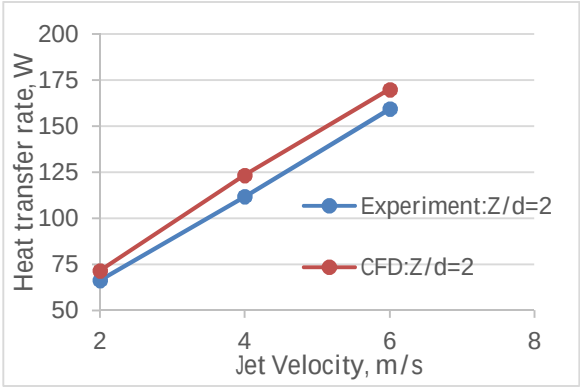

Figure 8: Comparison between the experimental and CFD simulations (Z/d = 2)

From the figure 8, it was evident that the predictions between the experiments and CFD simulations were in good agreement. For the Z/d = 2, closer agreements were observed at lower jet velocity configurations.

V. RESULTS AND ANALYSIS

With the validation between the experiments and numerical simulations were obtained, the CFD simulations for the remaining heat sink configurations were performed.

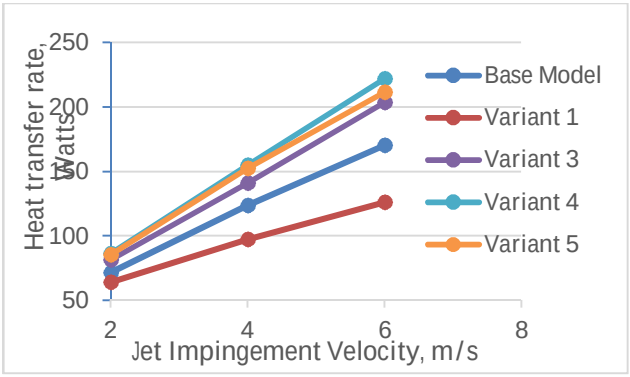

Figure 9: Heat Transfer rate comparisons for Z/d =2

Heat transfer rate from the Plate-finned (Variant-1) heat sink was observed to be lower than the Base Model (without any fins). This was consistently observed for Z/d =2, 4 and 6. The obstruction caused by the plate-fin for the movement of fluid had been attributed for this and could be seen in the following velocity contour plot.

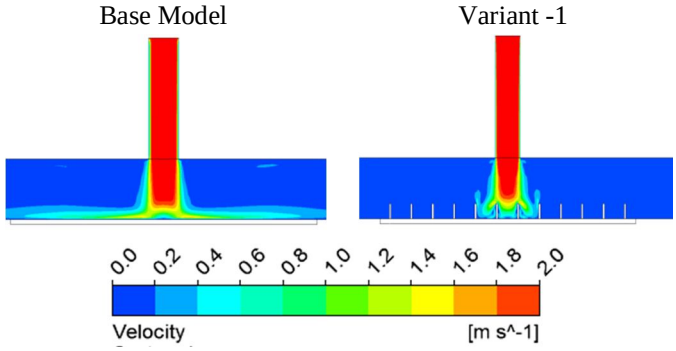

Figure 10: Velocity contours comparison between the Base Model and Variant-1

However, the pin-finned heat sink provides better fluid movement as compared to the plate-finned heat sink. A velocity vector plot for the pin-finned heat sink had been shown below.

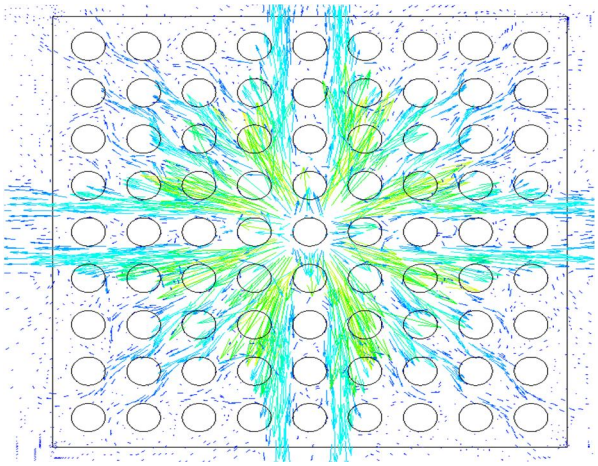

Figure 11: Velocity vector at mid-section for the Variant-3

As could be seen from the above figure, the lateral movement of fluid motion after the stagnation point shall be observed. The core pin-fins (near the impingement zone) receives higher fluid as compared to the pin-fins on the corners. Temperature contour comparison between the plate-finned and pin-finned heat sink had been shown in figure 12. For the variant-1, the fluid motion occurred only the three central channels while for the pin-finned heat sink received fluid motion almost throughout the heat sink. This resulted in higher heat transfer rate for the pin-finned heat sink as compared to the plate-finned heat sink.

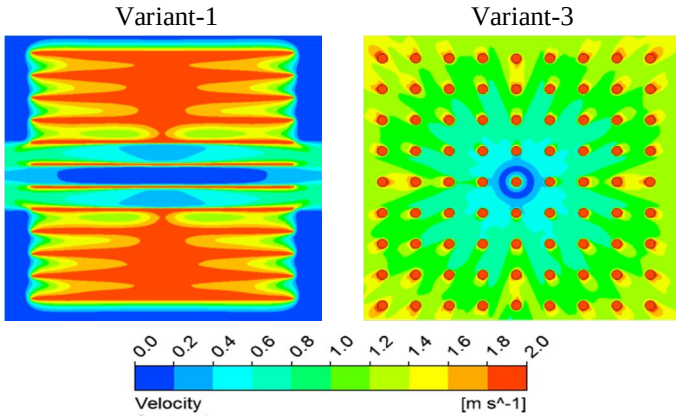

Figure 12: Temperature contours comparison between the Base Model and Variant 3

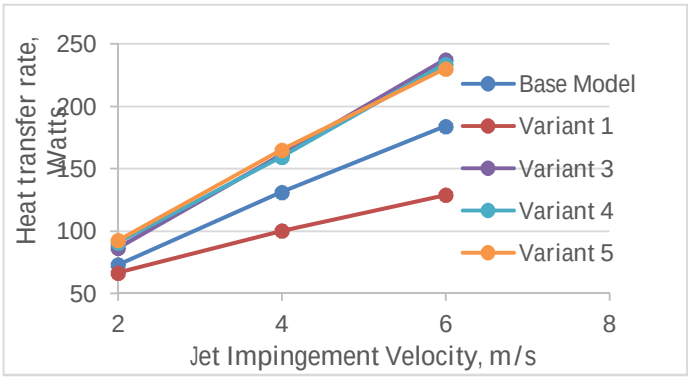

Figure 13: Heat transfer rate comparison among all heat sink variants for Z/d = 3

In the next phase of the work, the impact of pin-fin diameter over the heat transfer enhancement was studied. When the pin-fin diameter was increased from 10 mm (Variant 3) to 15 mm (Variant 4) to 20 mm (Variant 5), significant heat transfer enhancement was noted. This heat transfer enhancement was found to be independent of the nozzle-exit-to-the-impingement distance (Z/d) ratio. Expectedly, with the increase in the jet velocity, heat transfer rate was higher for the identical geometrical configurations.

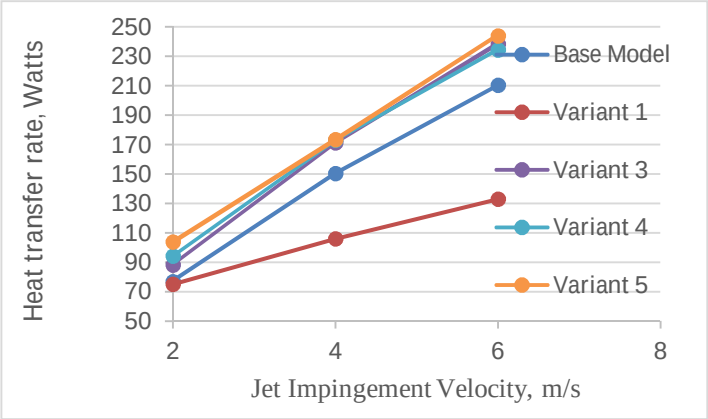

Figure 14: Heat transfer rate comparison among all heat sink variants for Z/d = 4

VI. CONCLUSIONS

Based on the results obtained from this study, the following conclusions were drawn.

A. For the impingement cooling, a good co-relation between the experiment and the CFD simulation methods could be achieved.

B. As compared to the Plate-finned heat sink, the Base Model heat sink without any fins was found to be providing higher heat transfer rate. This was attributed to the limited fluid path available for the plate-finned heat sinks

C. The pin-finned heat sinks had higher heat transfer rate among all the geometrical variants that were investigated in thi study. Nearly 25% of heat transfer enhancement was achieved for the pin- finned case (Variant-3, Jet velocity = 6 m/s) as compared to the Base Model. These are significant improvement in heat transfer rate.

D. The increase in the pin-fin diameter had a favorable influence over the heat transfer rate. This was independent of the nozzle-exit-to-the-impingement surface distance.

REFERENCES

[1] MdLokman H., RebeiBel F., Anders D. (2014), Multi-Jet Impingement Cooling of a Hot Flat Steel Plate, The 6th International Conference on Applied Energy,; Energy Procedia, Volume 61, pp 1835 – 183

[2] Yakut R.,Yakut K., Faruk Y, Altug K. (2016), Experimental and Numerical Investigations of Impingement Air Jet for a Heat Sink, IX International Conferencebon Computational Heat and Mass Transfer, Procedia Engineering, Volume 157, pp 3 – 12;

[3] Maghrabie H., Attalla M., Fawaz H., Khalil M. (2016), Numerical Investigation of Heat Transfer and Pressure Drop on In-Line Array of Heated Obstacles Cooled by Jet Impingement in Cross-Flow" Alexandria Engineering Journal.

[4] Sui D., Kim T., Xu M., Lu T. (2008), Flow and Heat Transfer Characteristics of Impinging Axial Fan Flows on a Uniformly Heated Flat Plate, International Journal of Transport Phenomena, Volume 10, pp 353 – 363;

[5] ChSastry M., Prasad B., Gupta A. (2015), Experimental and Computational Study of Fluid Flow on a Flat Plate with Three Rectangular Impinging SlotJets, Indian Journal of Engineering & Materials Sciences, Volume 22, pp 631 – 640;

[6] Zuckerman N., Lior N.(2006), Jet Impingement Heat Transfer: Physics, Correlations and Numerical Modeling, Advances in Heat Transfer, Volume 39, pp 565

[7] Huang J., Jang J.(2013), Numerical Study of a Confined Axisymmetric Jet Impingement Heat Transfer with Nanofluids, Scientific Research, Volume 5, pp 69-74;

[8] Behnia M., Ooi A. , Gregory (2005) P., Prediction of Turbulent Heat Transfer in Impinging Jet Geometries, WIT Transactions on State of the Art in Science and Engineering, Volume 15;

[9] Lemos M., Fischer C. (2008), Thermal Analysis of an Impingement Jet on a Plate with and without a Porous Layer, Numerical Heat Transfer, Part A, 54, pp 1022

[10] Jingzhou Z. , Chengfeng X. (2009), Numerical Study of Flow and Heat Transfer Characteristics of Impingement/Effusion Cooling, Chinese Journal of Hosain Aeronautics, Volume 22, pp 343 – 348

[11] M., Rebei B., Anders D. (2014), Multi-Jet Impingement Cooling of a Hot Flat Steel Plate, The 6th International Conference on Applied Energy, Energy Procedia, Volume 61, pp 1835 – 1839;

[12] Tahsini A., Mousavi S.(2012), Laminar Impinging Jet Heat Transfer for Curved Plates, International Journal of Mechanical Aerospace Industrial Mechatronic and Manufacturing Engineering, Volume 6, Number 12, pp 2788 – 2793;

[13] Xueqin B., Peng L., Lin G., Lizhan B., Wen D. (2015), Experimental Study of Jet Impingement Heat Transfer on a Variable Curvature Concave Surface in a Wing Leading Edge, International Journal of Heat and Mass Transfer, Volume 90, pp 92 – 101;

[14] Abdulla A., Janajreh I.(2015), Numerical Simulation of Turbine Blade Cooling via Jet Impingement, The 7th International Conference on Applied Energy, Energy Procedia, Volume 75, pp 3220 – 3229;
[15] Nayak S., Mishra P., Parashar S. (2016), Influence of Spray Characteristics on Heat Flux in Dual Phase Spray Impingement Cooling of Hot Surface, Alexandria Engineering Journal, Volume 55, pp 1995 – 2004;

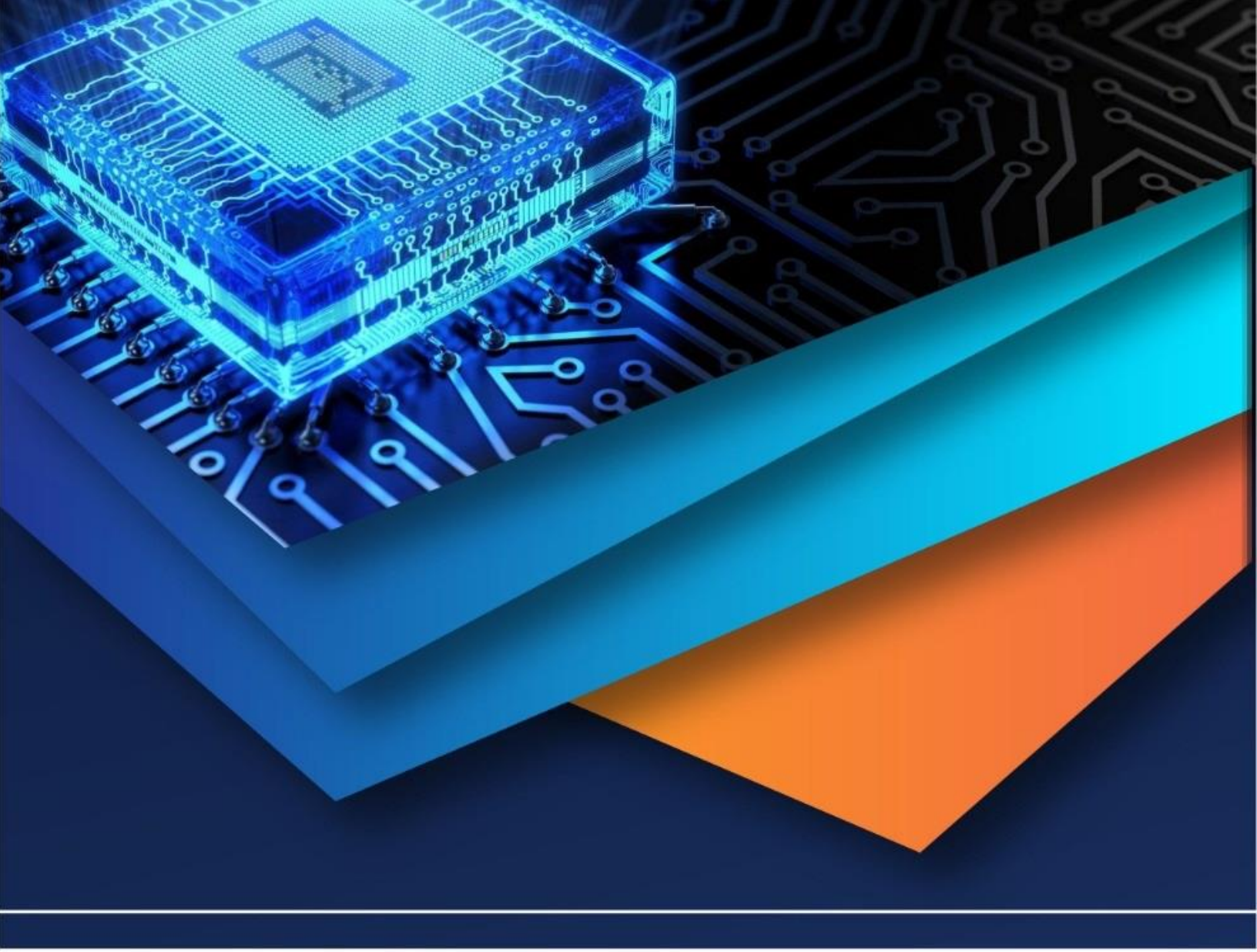

10.22214/IJRASET

45.98

IMPACT FACTOR: 7.129

IMPACT FACTOR: 7.429

INTERNATIONAL JOURNAL FOR RESEARCH

IN APPLIED SCIENCE & ENGINEERING TECHNOLOGY